Comparison of EPR-Visible Cu^{2+} Sites in pMMO from *Methylococcus capsulatus* (Bath) and *Methylomicrobium album* BG8

Sebastião S. Lemos,* Mary Lynne Perille Collins,† Sandra S. Eaton,‡ Gareth R. Eaton,‡ and William E. Antholine§

*Instituto de Química, Universidade de Brasília, Brasília-DF 70919-970, Brazil; †Department of Biological Sciences, University of Wisconsin-Milwaukee, Milwaukee, Wisconsin 53201 USA; ‡Department of Chemistry and Biochemistry, University of Denver, Denver, Colorado 80208 USA; and §Biophysics Research Institute, Medical College of Wisconsin, Milwaukee, Wisconsin 53226 USA

ABSTRACT X-band (9.1 GHz) and S-band (3.4 GHz) electron paramagnetic resonance (EPR) spectra for particulate methane monooxygenase (pMMO) in whole cells from *Methylococcus capsulatus* (Bath) grown on ^{63}Cu and ^{15}N were obtained and compared with previously reported spectra for pMMO from *Methylomicrobium album* BG8. For both *M. capsulatus* (Bath) and *M. album* BG8, two nearly identical Cu^{2+} EPR signals with resolved hyperfine coupling to four nitrogens are observed. The EPR parameters for pMMO from *M. capsulatus* (Bath) ($g_{\|} = 2.244$, $A_{\|} = 185$ G, and $A^N = 19$ G for signal one; $g_{\|} = 2.246$, $A_{\|} = 180$ G, and $A^N = 19$ G for signal two) and for pMMO from *M. album* BG8 ($g_{\|} = 2.243$, $A_{\|} = 180$ G, and $A^N = 18$ G for signal one; $g_{\|} = 2.251$, $A_{\|} = 180$ G, and $A^N = 18$ G for signal two) are very similar and are characteristic of type 2 Cu^{2+} in a square planar or square pyramidal geometry. In three-pulse electron spin echo envelope modulation (ESEEM) data for natural-abundance samples, nitrogen quadrupolar frequencies due to the distant nitrogens of coordinated histidine imidazoles were observed. The intensities of the quadrupolar combination bands indicate that there are three or four coordinated imidazoles, which implies that most, if not all, of the coordinated nitrogens detected in the continuous wave spectra are from histidine imidazoles.

INTRODUCTION

Methanotrophic bacteria use methane as their sole source of carbon and energy. These organisms oxidize methane by the following metabolic pathway:

$$CH_4 \xrightarrow{MMO} CH_3OH \rightarrow HCHO \rightarrow HCOOH \rightarrow CO_2$$
$$\downarrow$$
$$\text{biomass}$$

The first enzyme in the methane oxidation pathway is methane monooxygenase. Soluble (sMMO) and particulate (pMMO) forms of this enzyme occur. While sMMO shows a broad substrate specificity, pMMO is specific for substrates containing no more than five carbon atoms (Elliott et al., 1997). While pMMO is found in all known methanotrophs, sMMO is restricted to certain strains under conditions of copper stress. The structure and mechanism of sMMO are well understood (Rosenzweig et al., 1993; Lipscomb, 1994). Much less is known about pMMO.

The study of methane oxidation by methanotrophic bacteria is important for several reasons. These organisms constitute a biological sink for the greenhouse gas methane that has been increasing in the atmosphere. In addition, there are practical applications for methanotrophs, including stereospecific chemical catalysis. Methanotrophs also have application to bioremediation. In this regard, particular attention has been paid to the ability of both sMMO and pMMO to oxidize trichloroethylene (TCE), a priority pollutant (Alvarez-Cohen et al., 1992; DiSpirito et al., 1992; Hanson and Hanson, 1996; Little et al., 1988; Lontoh and Semrau, 1998; Oldenhuis et al., 1991). Molecular methods have been developed to detect methanotrophs in environmental samples, and these methods have been applied to TCE-contaminated sites (Cheng et al., 1999; Drought et al., 1999; Fode et al., 1999).

Understanding the function of methanotrophs in the environment, as well as exploiting them in various applications, requires a fundamental understanding of the metal centers. Moreover, the copper center(s) in pMMO may present an opportunity to investigate a previously unstudied type of catalytic center. The pMMO may also serve as a model for understanding ammonia monooxygenase (AMO), which has been suggested to be similar and evolutionarily related to pMMO (Holmes et al., 1995; Semrau et al., 1995a). Chan and collaborators have presented a mechanistic proposal for dioxygen reduction and methane activation by five to seven trinuclear copper clusters per pMMO molecule (Chan et al., 1993; Nguyen et al., 1996). DiSpirito and co-workers have presented an alternative model in which the catalytic site involves both iron and copper, although they reserve the option of a single ferrous iron center or an iron-iron center (Zahn and DiSpirito, 1996).

Methylomicrobium album BG8 is a well-studied methanotroph that has been the subject of investigations by us (Brantner et al., 1997, 2000; Collins et al., 1991; Yuan et al., 1997, 1998a,b, 1999) and by others (Arps et al., 1995; Berson and Lidstrom, 1997; Chistoserdova et al., 1994; McPheat et al., 1987). We have identified a pMMO-specific electron paramagnetic resonance (EPR) signal in *M. album*

Received for publication 16 December 1999 and in final form 22 April 2000.

Address reprint requests to Dr. William E. Antholine, Biophysics Research Institute, Medical College of Wisconsin, 8701 Watertown Plank Rd., Milwaukee, WI 53226. Tel.: 414-456-4032; Fax: 414-456-6512; E-mail: wantholi@mcw.edu.

0006-3495/00/08/1085/10 $2.00

BG8 that is similar to that observed by others in *Methylococcus capsulatus* (Bath) (Nguyen et al., 1994, 1996; Zahn and DiSpirito, 1996) and *Methylosinus trichosporium* OB3b (Takeguchi et al., 1998a,b, 1999). The amino acid sequence is available for pMMO from *M. capsulatus* (Bath) (GenBank, accession nos. L40804 (copy 1) and U94337 (copy 2)) and not from *M. album* BG8. We are using EPR spectroscopy to compare the Cu^{2+} binding sites in *M. capsulatus* (Bath) and *M. album* BG8.

We have shown that resolution of the Cu^{2+} EPR signal for pMMO in intact *M. album* BG8 cells isotopically enriched in ^{63}Cu and ^{15}N ($I = ½$) is substantially better than in natural-abundance samples. The natural-abundance samples contain ~2:1 ratios of ^{63}Cu:^{65}Cu and predominantly ^{14}N ($I = 1$) (Yuan et al., 1999). We now compare the X-band and S-band, continuous wave, EPR spectra of pMMO in intact *M. capsulatus* (Bath) cells isotopically enriched with ^{63}Cu and ^{15}N with our previously reported results for *M. album* BG8. In addition, to better characterize the nitrogen-containing ligands that are coordinated to the Cu^{2+}, we have obtained two-pulse and three-pulse electron spin echo data for natural-abundance and isotopically enriched samples of both organisms.

MATERIALS AND METHODS

Growth of bacterium

M. capsulatus (Bath) and *M. album* BG8 cells were grown in batch culture in nitrate mineral salts (NMS) medium (Whittenbury et al., 1970) containing 5 or 10 μM cupric sulfate for *M. capsulatus* (Bath) and 5 μM cupric sulfate for *M. album* BG8. Cultures were incubated at 30°C with shaking at 150 rpm in a 50% methane, 50% air (v/v) atmosphere. Cells cultured under these conditions have MMO activity measured by propylene oxidation >20 nmol/min/mg protein (Nguyen et al., 1994; Zahn and DiSpirito, 1996; Yuan et al., 1999). Cells were harvested by centrifugation at 6000 rpm for 40 min at 4°C. The cell pellets were washed twice in ice-cold 20 mM phosphate, 5 mM magnesium chloride buffer (pH 7) and collected at 10,000 rpm for 10 min. For isotope enrichment studies, cells were grown in the same medium by the same process, except that potassium nitrate was replaced by ^{15}N-potassium nitrate (98 atom % ^{15}N; Aldrich, Milwaukee, WI), and cupric sulfate was replaced by ^{63}Cu-cupric nitrate (99.9% ^{63}Cu; Cambridge Isotope Laboratories, Andover, MA). Because the latter compound contributed less than 0.2% of the nitrate in the medium, the isotopic purity of the ^{15}N after the addition of ^{63}Cu was 97.8%.

EPR measurements

EPR spectra were obtained as previously described (Yuan et al., 1999). In brief, X-band spectra at 77 K were recorded on a Varian E109 Century Series spectrometer with a Varian TE102 cavity (Varian, Palo Alto, CA) at the Medical College of Wisconsin. X-band spectra at 60 K were obtained on a Bruker Elexsys E580 with a split-ring resonator and an Oxford ESR935 cryostat at the University of Denver. S-band (3.4 GHz) spectra were obtained on a spectrometer with a loop-gap resonator and a low-frequency microwave bridge built at the National Biomedical EPR Center, Medical College of Wisconsin. EPR parameters were obtained by analysis of the spectra as reported previously (Yuan et al., 1999).

ESEEM measurements

Two-pulse and three-pulse electron spin echo envelope modulation (ESEEM) experiments were performed at 10 K with a Bruker Elexsys E580 spectrometer and split-ring resonator at the University of Denver. Two-pulse ESEEM data were obtained with a 90°-τ-180°-τ-echo sequence, an initial τ value of 80 ns, and 1024 steps of 6 ns. The length of a 90° pulse was 16 ns. Three-pulse ESEEM data were obtained with a 90°-τ-90°-T-90°-τ-echo sequence with the τ value selected to suppress proton modulation. The initial value of T was 320 ns, and data were recorded for 1024 steps of 24 ns. ESEEM spectra were obtained by cosine Fourier transformation, using the dead-time reconstruction method of Mims (1984).

RESULTS AND DISCUSSION

X-band EPR spectra from *M. capsulatus* (Bath) and *M. album* BG8

The type 2 Cu^{2+} EPR signals in *M. capsulatus* (Bath) cells and *M. album* BG8 cells grown on natural-abundance media are shown in Fig. 1, *A* and *B*, respectively. The resolution of the perpendicular region of the spectrum is greater for *M. album* than for *M. capsulatus*, but the overall features are very similar. The assignment of these spectra to Cu^{2+} in pMMO is based on the similarity of these spectra to those obtained with purified preparations of pMMO from *M. capsulatus* (Bath) (Nguyen et al., 1994), *M. trichosporium* OB3b (Takeguchi et al., 1998b), and *M. album* BG8 (Lemos et al., unpublished data). It is not unexpected that pMMO

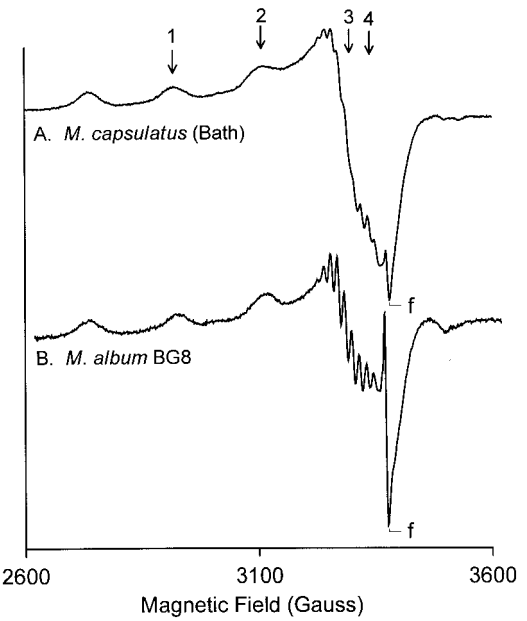

FIGURE 1 X-band EPR spectra of cells grown with natural-abundance isotopes. (*A*) *M. capsulatus* (Bath) cells grown in 10 μM Cu and (*B*) *M. album* BG8 cells grown in 5 μM Cu. Numbered arrows pointing down indicate field positions for ESEEM data. Spectrometer conditions: microwave frequency, 9.4 GHz; modulation amplitude, 4 G; microwave power, 0.25 mW; temperature, 60 K. The sharp signal marked with an f is due to a free radical that is present in varying concentrations in the cells.

would dominate the EPR spectrum of whole cells, because pMMO is the major membrane protein in these membranes (Collins et al., 1991).

About 500 μM Cu^{2+} is detected by EPR in *M. album* BG8 and *M. capsulatus* (Bath) cells when compared to a 1 mM cupric perchlorate standard solution. The concentration of the type 2 Cu^{2+} signals detected by EPR is correlated to the pMMO concentration (Nguyen et al., 1994; Semrau et al., 1995b). Nevertheless, some percentage due to apo pMMO and fully reduced pMMO has not been considered with the EPR measurements.

The $g_\perp$ region of the X-band EPR spectra for *M. capsulatus* (Bath) cells grown on the single isotopes ^{63}Cu and ^{15}N (Fig. 2, *A* and *B*) is better resolved than in spectra for natural-abundance samples (Fig. 1 *A*). The improved resolution is due to the presence of a single copper isotope (instead of two), and the change from ^{14}N ($I = 1$) to ^{15}N ($I = 1/2$), which decreases the number of nitrogen super-hyperfine lines and increases the nitrogen hyperfine coupling constant by 40%. In some preparations a weaker Cu^{2+} signal, indicated by the arrows pointing up in Fig. 2 *B*, in addition to a broad underlying signal (see *filled circle* and *sloping baseline* in Fig. 2) and a high field signal (see *filled diamond* in Fig. 2) are superimposed on the type 2 Cu^{2+} signal.

The X-band spectra for isotopically enriched pMMO from *M. album* BG8 (Fig. 2 *C*) are better resolved and have less underlying signal than the spectra for pMMO from *M. capsulatus* (Bath) cells (Fig. 2, *A* and *B*), which makes the spectrum from *M. album* BG8 easier to interpret. Expansion of the low field $M_I = -3/2$ line for *M. album* BG8 (Fig. 3 *C*) shows a six-line splitting pattern that is attributed to overlapping five-line signals from two Cu^{2+} complexes bound to four approximately equivalent ^{15}N donor atoms (Yuan et al., 1999). These two signals are not resolved in cells grown in media with natural isotope abundance (Fig. 1). Although the six-line splitting is not as well resolved in the expansion of the $M_I = -3/2$ line for pMMO from *M. capsulatus* (Bath) (Fig. 3, *A* and *B*) as for *M. album* BG8 (Fig. 3 *C*), the similarity in the lineshapes suggests that the splitting patterns are similar. Analysis of the spectra gave similar parameters for the two organisms (Table 1). The difference in $g_\parallel$ of 0.002 for the two signals in *M. capsulatus*

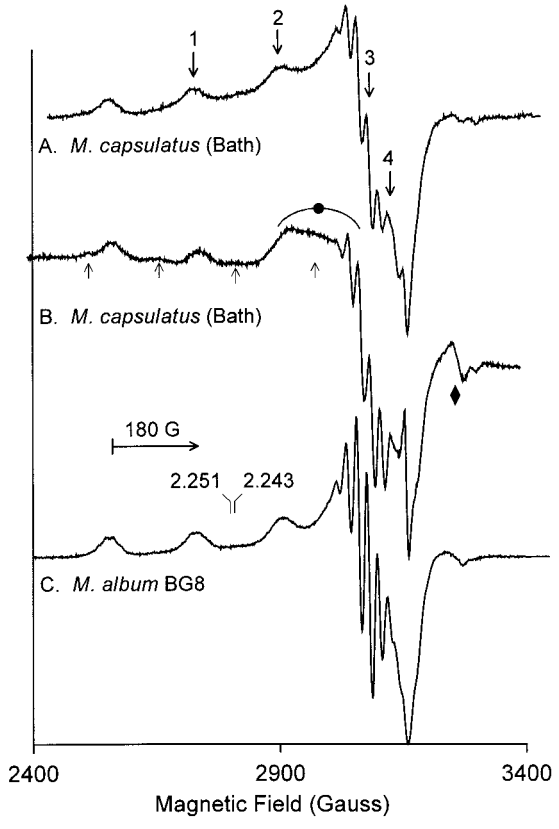

FIGURE 2 X-band EPR spectra of cells grown with ^{15}N and $^{63}Cu^{2+}$. (*A*) *M. capsulatus* (Bath) cells grown in 5 μM Cu and (*B*) 10 μM Cu and (*C*) *M. album* BG8 cells grown in 5 μM Cu. Numbered arrows pointing down indicate field positions for ESEEM data. Arrows pointing up indicate lines for a minor Cu^{2+} species. A filled circle with an arc and the sloping baseline mark the broad underlying signal; a filled diamond marks the high field signal. Spectrometer conditions: microwave frequency, 9.0 GHz; modulation amplitude, 5 G; microwave power, 5 mW; temperature, 77 K; number of scans, four.

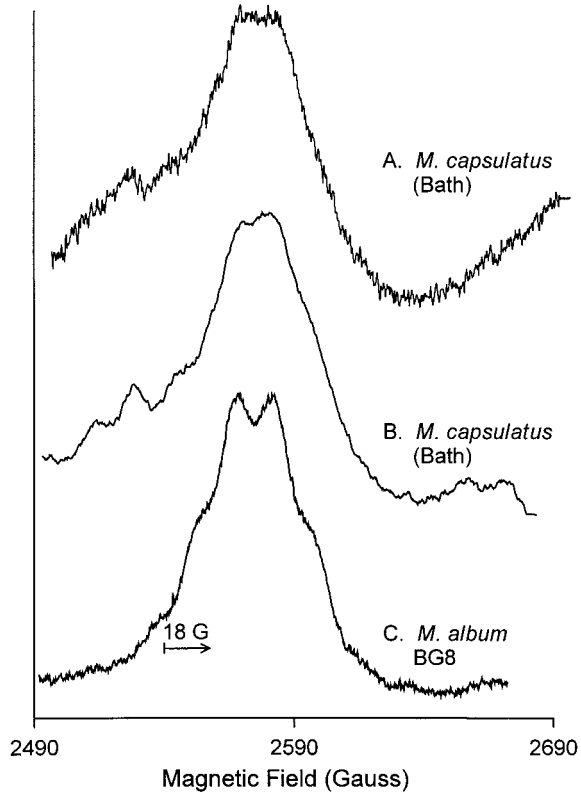

FIGURE 3 Expansion of the $M_I = -3/2$ line in the $g_\parallel$ region of X-band spectra. (*A*) *M. capsulatus* (Bath) cells grown in 5 μM Cu and (*B*) 10 μM Cu, and (*C*) *M. album* BG8 cells grown in 5 μM Cu. Spectrometer conditions are as in Fig. 2, except that 16 scans were averaged.

TABLE 1 EPR parameters for type 2 Cu^{2+}

Sample	$A_{\parallel}$ (G)	$g_{\parallel}$	$g_{\perp}$	A^{N} (G)*	No. of equivalent nitrogens	Reference
M. capsulatus (Bath) in cells						
^{63}Cu, ^{15}N signal 1	185	2.244	2.070	19 (^{15}N)	4	This work
^{63}Cu, ^{15}N signal 2	180	2.246	2.070	19 (^{15}N)	4	
^{63}Cu, ^{15}N minor signal	150	2.31	—	15 (^{15}N)	1	
M. capsulatus (Bath) in membranes (natural isotope abundance)	180	2.25	2.058	~15 (^{14}N)	—	Nguyen et al. (1994)
M. capsulatus (Bath) in purified protein (natural isotope abundance)	(similar to type 2 site in membranes)					Nguyen et al. (1998)
M. album BG8 in cells						
^{63}Cu, ^{15}N signal 1	180	2.243	2.067	18 (^{15}N)	4	Yuan et al. (1999)
^{63}Cu, ^{15}N signal 2	180	2.251	2.067	18 (^{15}N)	4	
^{63}Cu, ^{14}N	185	2.243	—	13 (^{14}N)	3 or 4	Yuan et al. (1997)
M. trichosporium OB3b (natural isotope abundance) in membranes and purified	184	2.24	2.06	14.5 (^{14}N)	—	Takeguchi et al. (1998a,b)

*Based on $M_I = -1/2$ line in $g_{\parallel}$ region at S-band, the $M_I = -3/2$ line at X-band, or the $g_{\perp}$ region if resolution of the $g_{\parallel}$ region was inadequate.

(Bath) is less than the difference of 0.008 for pMMO from *M. album* BG8. $A_{\parallel}$ values are different for the two Cu^{2+} complexes in *M. capsulatus* (Bath), but nearly the same for the two Cu^{2+} complexes in *M. album* BG8. Nevertheless, the differences are small, and the overall conclusion is that the Cu^{2+} binding environments in pMMO are very similar for the two organisms.

S-band EPR spectra from *M. capsulatus* (Bath) and *M. album* BG8

S-band (3.4 GHz) spectra for pMMO in *M. capsulatus* (Bath) cells grown on ^{63}Cu and ^{15}N were obtained to take advantage of the better resolution of the nitrogen superhyperfine structure at low frequencies (Rahkit et al., 1985; Yuan et al., 1997, 1999). Splittings due to ^{15}N ($I = 1/2$) are well resolved in both the $g_{\parallel}$ and $g_{\perp}$ regions of the S-band spectra (Figs. 4 *A* and 5 *A*). The best resolution is observed for the $M_I = -1/2$ line in the $g_{\parallel}$ region (Fig. 5 *A*). Although the baseline of the spectrum for pMMO from *M. capsulatus* (Bath) is distorted because of a broad underlying signal (Fig. 4 *A*), the spectrum is similar to that obtained for pMMO from *M. album* BG8 at S-band frequencies (Figs. 4 *B* and 5 *B*). For both samples the lines from the two very similar cupric complexes that were partially resolved for $M_I = -3/2$ at X-band (Figs. 2 *A* and 3 *A*) are approximately superimposed at S-band (Figs. 4 *A* and 5 *A*). The frequency dependence of the splitting pattern is consistent with the assignment of the six-line pattern at X-band to two overlapping five-line patterns separated by *g*-value differences.

The EPR parameters given in Table 1 were obtained by analysis of the X-band and S-band data. These parameters are characteristic of Cu^{2+} in an approximately square planar or square pyramidal coordination environment (Vänngård, 1972).

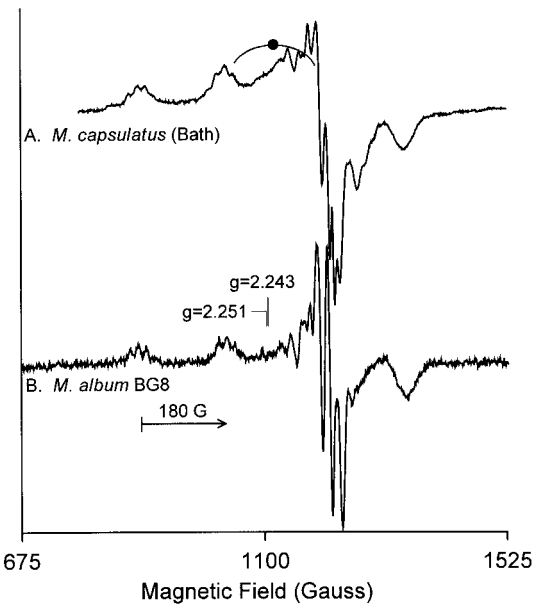

FIGURE 4 S-band EPR spectra of cells grown with ^{15}N and $^{63}Cu^{2+}$. (*A*) *M. capsulatus* (Bath) cells grown in 10 μM Cu and (*B*) *M. album* BG8 cells grown in 5 μM Cu. A filled circle with an arc marks the broad underlying signal. Spectrometer conditions: microwave frequency, 3.45 GHz; modulation amplitude, 5 G; microwave power, (*A*) 16 dB and (*B*) 22 dB, 0.063 mW; temperature, 133 K; number of scans, four.

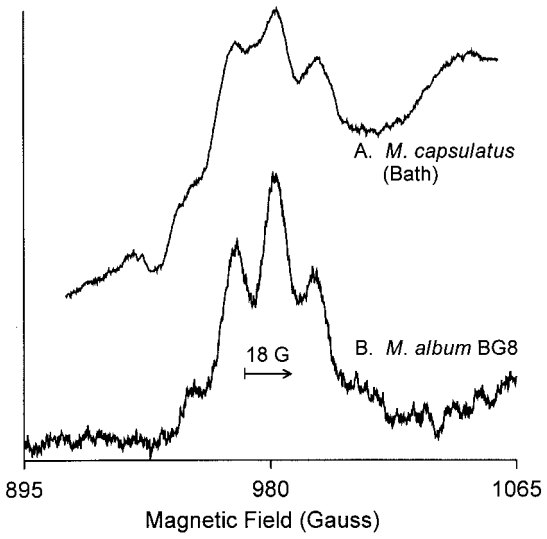

FIGURE 5 Expansion of the $M_I = -1/2$ line in the $g_{\|}$ region of S-band spectra. (*A*) *M. capsulatus* (Bath) cells grown in 10 μM Cu and (*B*) *M. album* BG8 cells grown in 5 μM Cu. Spectrometer conditions are as in Fig. 4, except that 16 scans were averaged.

Conclusions from X-band and S-band CW spectra

The dominant EPR-detectable Cu^{2+} signals from pMMO are composed of two very similar spectra in *M. capsulatus* (Bath) and *M. album* BG8 cells. These signals can be resolved for cells grown on isotopically enriched ^{63}Cu and ^{15}N. Comparison of X-band and S-band spectra facilitates determination of the EPR parameters, which are characteristic of type 2 Cu^{2+} in a square planar or square pyramidal configuration. The EPR parameters and the nitrogen hyperfine splitting patterns indicate that the Cu^{2+} is bound to four nitrogens with nearly identical hyperfine coupling constants.

ESEEM data for pMMO in *M. capsulatus* (Bath) and *M. album* BG8

Natural isotope abundance

The CW spectra of the intact cells clearly show that four nitrogens are coordinated to the Cu^{2+} in pMMO. The next step in defining the coordination site is to determine what types of nitrogenous ligands are involved. ESEEM is a powerful technique for identifying and characterizing nuclear spins that are weakly coupled to a paramagnetic center (Dikanov et al., 1992). In particular, the distant (nonbonded) nitrogens of coordinated histidine imidazoles give distinctive ^{14}N ESEEM frequencies. The magnitude of the nuclear quadrupole interactions, nuclear Zeeman interactions, and the nuclear hyperfine interactions for the nonbonded nitrogens of the imidazoles are all approximately equal. The ESEEM spectrum results from the effective cancellation of the nuclear Zeeman and hyperfine energies in one m_s manifold for ^{14}N. The observation of these distinctive ESEEM frequencies can be used to distinguish coordinate imidazoles from other nitrogen donor ligands.

Three-pulse ESEEM data were collected at the magnetic fields indicated by the arrows in Fig. 1. Fourier transforms of the ESEEM data at field position 3, in the $g_{\perp}$ region of the spectra, are shown in Fig. 6. The spectra are strikingly similar for *M. capsulatus* (Bath) and *M. album* BG8. The ^{14}N ESEEM frequencies (Table 2) were assigned as follows. The peaks between 0.5 and 1.6 MHz showed little dependence on magnetic field and are characteristic of the quadrupole frequencies for the distant nitrogen of coordinated imidazole (Mims and Peisach, 1978; Dikanov et al., 1992). The observation of more than three quadrupolar frequencies between 0.5 and 1.6 MHz could arise from incomplete orientation selection. However, multiple peaks are observed even at the highest field (*position 4*, Fig. 1), where the data are expected to be relatively orientation selective. The data are consistent with either inequivalence of the nitrogens or the existence of two Cu^{2+} complexes, or both. The frequencies between 2.3 and 3.2 also show little field dependence and are equal to the sums of quadrupolar frequencies. These combination frequencies are present when more than one imidazole is bound to the same Cu^{2+} (Lu et al., 1992). The frequencies of the peaks at 3.8–4.2 MHz increased as a function of magnetic field and were therefore assigned as double-quantum peaks. The frequen-

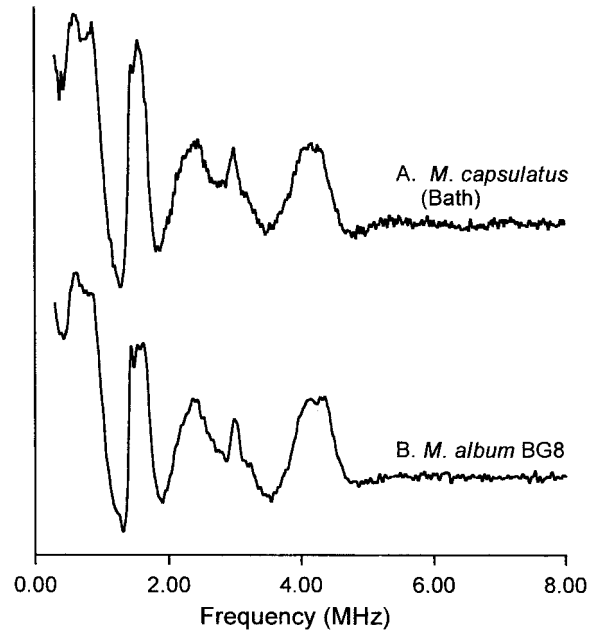

FIGURE 6 Cosine Fourier transform of three-pulse ESEEM data obtained at position 3 (Fig. 1), which is in the $g_{\perp}$ region for Cu^{2+} sites in *M. capsulatus* (*A*) and *M. album* BG8 (*B*) cells. Instrument conditions: microwave frequency, 9.4 GHz; temperature, 10 K; constant time τ selected to minimize proton modulation, 142 ns; shot repetition time, 5.1 ms; data points collected, 1024; length of Fourier transform, 4096.

TABLE 2 ^{14}N ESEEM frequencies (MHz) at X-band (9.45–9.46 GHz)

Field position (Fig. 1)	Quadrupolar frequencies	Quadrupolar combination frequencies	Double-quantum frequencies
M. capsulatus (Bath)			
1	0.6, 0.8, 1.53	2.4, 3.0	3.8
2	0.61, 0.78, 1.58	2.4, 3.0	4.0
3	0.56, 0.80, 1.44, 1.52	2.4, 3.1	4.2
4	0.60, 0.80, 1.42, 1.53	2.4, 3.2	4.3
M. album BG8			
1	0.63, 0.85, 1.49	2.3	3.8
2	0.66, 0.78, 1.50, 1.58	2.4, 3.1	4.0
3	0.63, 0.78, 1.42, 1.60	2.4, 3.2	4.2
4	0.61, 0.80, 1.41, 1.52	2.4, 3.1	4.2

cies observed in two-pulse ESEEM were consistent with the three-pulse data, but the lines are broader in the two-pulse ESEEM, so frequencies are less well defined.

The intensities of the quadrupolar combination bands increase as the number of coordinated imidazoles increases (Lu et al., 1992). Based on comparison of the intensities of the quadrupolar combination bands observed for pMMO in intact cells (Fig. 6) with ESEEM spectra of samples that are known to contain one, two, or four imidazoles (Lu et al., 1992), we conclude that there are at least three and possibly four histidine imidazoles bound to the Cu^{2+} in pMMO from both *M. capsulatus* (Bath) and *M. album* BG8. In contrast, the relative intensities of the combination lines in purified pMMO from *M. capsulatus* (Bath) (Elliott et al., 1998; Takeguchi et al., 1999) are consistent with the binding of only two imidazoles to Cu(II). Whether the binding of some imidazoles is lost upon purification or the data for the purified enzymes are from the superposition of Cu(II) signals and therefore give an average value is not clear. Under our isolation conditions, if H_2O_2 is added to pMMO in membrane fractions, the resulting ESEEM data are consistent with the binding of a single imidazole to pMMO (data not shown, work in progress). It may be that there is a partial loss of Cu^{2+}-bound imidazoles upon treatment with H_2O_2 or as a result of attempts to purify pMMO from cells. The activity of pMMO decreases ~10-fold upon purification (Elliott et al., 1998). This ESEEM result is the first indication that change in structure at the Cu^{2+} site may be correlated with loss of activity.

Isotopically enriched samples

For samples grown on ^{63}Cu and ^{15}N, two- and three-pulse ESEEM data were recorded at the magnetic fields indicated in Fig. 2. Well-defined ^{15}N modulation frequencies were obtained from the two-pulse echoes. ν_α was the only frequency that was well defined in the three-pulse experiments. (The two basic ^{15}N nuclear modulation frequencies are ν_α and ν_β.) The ^{15}N frequencies are very similar to those reported by Dikanov et al. (1994b) for coupling to the distant nitrogens in $[Cu(^{15}N\text{-imH})_4]^{2+}$, where imH is imidazole. The frequencies reported in Table 3 were assigned as described by Dikanov et al. (1994b). For copper-imidazole complexes, the anisotropic contribution, B, to the electron-^{15}N coupling of the distal nitrogen is smaller than the isotropic coupling, A, and so A can be estimated from the expression $A \approx 2*(\nu_\beta - \nu_I)$, where ν_I is the ^{15}N resonance frequency at that observing field. Based on this approximation, an average value for the distal nitrogen superhyperfine coupling, A, across the spectrum is 2.5–2.6 MHz (Table 3), which is likely to be close to the isotropic value. Dikanov et al. (1994b) reported $A = 2.44$ MHz for the distal nitrogen of coordinated ^{15}N-imidazole. The similarity between their value and the value of 2.5 MHz for pMMO is consistent with assignment of the ^{15}N modulation to histidine imidazole bound to Cu^{2+} in pMMO. Within the limited resolution of the two-pulse ESEEM data, only one nitrogen binding environment is observed.

Conclusions from ESEEM data

Both ^{14}N and ^{15}N ESEEM frequencies for all of the pMMO samples are similar to what has been observed for the remote nitrogen of coordinated histidine imidazole in Cu^{2+} samples. These nitrogen ESEEM frequencies are similar for the two organisms, which indicates that there is substantial similarity in the nitrogens coordinated to the copper in the two samples. The frequencies are not identical, and the Cu^{2+}-nitrogen interactions are somewhat different for pMMO from different organisms. (This is in agreement with the EPR parameters from multifrequency data in Table 1.) The substantial intensity of the quadrupolar combination frequencies for samples of cells from both organisms indicates that there are more than two bound histidines, but whether three or four histidines interact with Cu^{2+} is not determined. There is no evidence in the electron spin echo data for nitrogen, other than the remote nitrogen of coordinated histidine.

TABLE 3 ^{15}N ESEEM frequencies (MHz) at X-band (9.45–9.46 GHz)

Field (Fig. 2)	ν_α	$\nu_\alpha - \nu_\beta$	ν_β	$\nu_\alpha + \nu_\beta$	ν_I	A
M. capsulatus (Bath)						
1		2.06	2.40	2.75	1.26	2.3
2		2.00	2.51	2.89	1.34	2.3
3		2.17	2.72	3.10	1.41	2.7
4	~0.3	2.30	2.78	3.15	1.45	2.7
M. album BG8						
1		2.07	2.47	2.82	1.26	2.4
2		2.10	2.59	2.98	1.34	2.5
3	~0.2	2.15	2.76	3.08	1.41	2.7
4	0.24	2.21	2.81	3.21	1.45	2.7

TABLE 4 Copper-imidazole ligation by N_ε or N_δ

Protein	No. of histidines	Cu-N_δ	Cu-N_ε	Pattern	Reference
Amine oxidase (active)	3	1	2	N_ε H431XH433; N_δ H592	Wilce et al. (1997)
Ascorbate oxidase (red.)	3 (Cu2)	—	3	N_ε H104XH106	Messerschmidt (1993)
	3 (Cu3)	1	2	N_ε H506XH508	
	2 (Cu4)	—	2	N_ε/N_δ H60XH62	
Cytochrome *c* oxidase	3 (Cu_B)	1	2	N_ε H325H326; N_δ H276	Iwata et al. (1995)

Role of Cu^{2+} site in pMMO

In addition to the quantitation discussed above, several observations have led us to associate the Cu^{2+} EPR signal with active pMMO. Our prior studies suggest that the EPR-detectable Cu^{2+} site is a good reporter for the concentration of Cu^{2+} bound to pMMO (Yuan et al., 1998a,b). In other preliminary work not shown, EPR-detectable Cu^{2+} can be reconstituted in pMMO by the addition of Cu^{2+} to partially purified preparations. When oxidizing equivalents of hypochlorite are added to partially purified pMMO preparations, the EPR-detectable Cu^{2+} increases slowly (4–6 h, 0°C), and then it decreases overnight at 0°C. The eventual decrease indicates that reducing equivalents are present in the partially purified preparations. Other data suggest that the EPR-detectable signal correlates with enzyme activity (Nguyen et al., 1994; Semrau et al., 1995b). Two signals from *M. capsulatus* (Bath) at low temperatures are superimposed, one signal from two unresolved type 2 Cu^{2+} and the other a broad signal at $g = 2.1$. It is hypothesized that the broad signal may correlate with activity (Semrau et al., 1995b). The combined EPR data for the two type 2 Cu^{2+} suggest that four nitrogen donors are coordinated in the equatorial plane of the Cu^{2+} site, which is not typical for catalytic copper sites (Wilce et al., 1997). This coordination geometry does not provide an easily replaceable equatorial ligand, although a substrate might bind in an axial position. Alternatively, binding Cu^{2+} to this site may stabilize the protein structure and enhance its activity. Little is known about the redox potential for this Cu^{2+} site, so it is too soon to speculate whether this site could be used to transfer electrons to the active site. In summary, it is too soon to speculate about whether the EPR-detectable type 2 Cu^{2+} sites are primarily used to stabilize protein structure, to provide a conduit to the redox active center, or as a component of the active center.

Possible binding sites for type 2 Cu^{2+} in pMMO

The combined CW and ESEEM data for pMMO indicate that there are four nitrogens coordinated to the Cu^{2+} and that three or four of these nitrogens are histidine imidazoles. In Table 4 we have summarized information concerning Cu^{2+} coordination sites in proteins that bind Cu^{2+} via multiple histidines. To our knowledge, the binding of four nitrogens and three or four almost equivalent imidazoles makes the pMMO site unique for nonporphyrin cupric complexes in a protein. The Cu^{2+} site in superoxide dismutase (SOD) also has four imidazoles bound to Cu^{2+}, but the EPR parameters, particularly the $A_\parallel$ value of 139 G and $g_\parallel = 2.265$, distinguish the Cu^{2+} site in SOD from that in pMMO. Two possible sites for Cu^{2+} in pMMO are as follows:

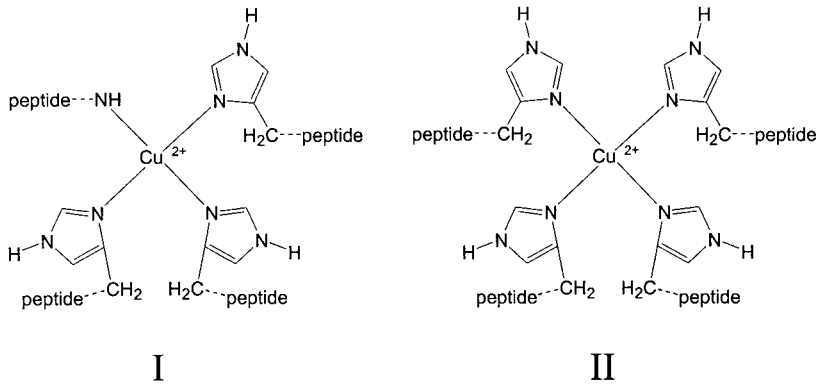

I II

Schematic for the proposed binding sites for type 2 Cu^{2+} in pMMO.

The above structures are drawn with a δ nitrogen from imidazole bound to copper, but either the δ or ε nitrogen is used to bind copper to histidine imidazole in proteins (Table 4). Whether ε or δ nitrogen binds to copper often depends on the folding of the protein. If the N-terminal amine nitrogen is not a donor atom for the equatorial plane, a peptidyl-nitrogen atom might be involved as a donor atom for the EPR-detectable site of pMMO, as depicted for the proposed binding site (I).

The possibility of a bridging imidazole between the EPR-detectable Cu^{2+} and a second metal ion, as in SOD, merits consideration. The nitrogen ESEEM frequencies for the pMMO samples are not split in the way that would be predicted for bridging to a diamagnetic M^{2+} metal (Fee et al., 1981). If an imidazole bridged two Cu^{2+} sites, the EPR spectrum would be expected to show hyperfine splitting to two Cu nuclei, which is not observed, or the pair might be EPR silent. If an imidazole bridged the Cu^{2+} and Fe^{2+}, enhanced electron spin-lattice relaxation of the Cu^{2+} would be expected. The spin-lattice relaxation time for the Cu^{2+} in pMMO from *M. capsulatus* (Bath) obtained by long-pulse saturation recovery decreases from ~2 ms at 15 K to 10 μs at 50 K. These values are in the range expected for approximately C_{4v} symmetry Cu^{2+} (Zhou et al., 1999) and are not consistent with interaction with a rapidly relaxing Fe center. Literature values of nitrogen ESEEM frequencies are not known to us for an imidazole bridging between Cu^{2+} and a diamagnetic M^{+} metal. If an imidazole were bridging Cu^{2+} and Cu^{+}, one would expect to see changes in the copper hyperfine splitting if the site were mixed valence (i.e., effective oxidation state of +1.5 for both Cu), but little change for a trapped valence Cu^{2+}-Cu^{+} site, so the possibility of trapped-valence Cu^{2+}-Cu^{+} cannot be ruled out.

The dominant contributions to the EPR spectra are due to two very similar copper environments. These could be two distinct binding sites or two slightly different forms of the same binding site. If there are two sites composed of either three or four nitrogen donor atoms from histidine imidazoles, six to eight histidines would be needed to form the two binding sites. If there is only one type 2 Cu^{2+} binding site in pMMO, only three or four histidines are needed. There are seven histidines in the 47-kDa subunit, of which six are conserved between pMMO from *M. capsulatus* (Bath) and AMO from *Nitrosomonas europaea*; five histidines in the 27-kDa subunit, of which three are conserved; and five histidines in the 25-kDa subunit. Typical patterns for strong chelation of Cu^{2+} such as . . .HXXH. . . are absent from pMMO. Copper-containing amine oxidases bind Cu^{2+}, using . . .HXH. . . plus a third histidine and two water molecules in a square pyramidal arrangement (Wilce et al., 1997). There is a . . .HXH. . . sequence in both the 47-kDa and the 27-kDa subunits. Both sites would need to be completed with two additional nitrogen donors; one or two of these nitrogens are from imidazole. The 47-kDa subunit (pmoB) has His as an N-terminal residue. It is hypothesized that this residue provides an adequate chelate ligand for Cu^{2+} through its N-terminal amine nitrogen and the imine nitrogen from imidazole (Yuan et al., 1999). If this segment is bound, the two additional ligands would both have to be histidine imidazoles.

On the other hand, the . . .HXH. . . sequence is known to support binding of trinuclear copper sites, and two of the coppers from these sites are EPR silent. For example, four . . .HXH. . . sequences form an EPR-detectable Cu^{2+} and an EPR antiferromagnetically coupled Cu^{2+} in the oxidized state and Cu^{+} in the reduced state in laccase and ascorbate oxidase (Holm et al., 1996, and references therein). There are not enough . . .HXH. . . sequences in pMMO to mimic the centers in laccase and ascorbate oxidase. Therefore, if . . .HXH. . . is involved in binding dinuclear copper, the structure will be different from that described for laccase or ascorbate oxidase. The previous discussion is based on the hypothesis that each copper site is formed from a single subunit. If they are not, more combinations are possible.

While there are two copies for pMMO in the gene (GenBank, accession nos. L40804 (copy 1) and U94337 (copy 2)), there is only one amino acid residue that varies between pmoA1 (Asn^{173}) and pmoA2 (Tyr^{173}), or between pmoB1 (Ser^{385}) and pmoB2 (Arg^{385}), or between pmoC1 (Arg^{239}) and pmoC2 (Ser^{239}). How such a subtle change would account for different EPR signals is not clear, so the two copies are assumed not to account for the two very similar, but distinguishable, type 2 Cu^{2+} signals. If the Cu^{2+} binding site is formed from three imidazoles or if the imidazoles are inequivalent (for example, δ and ε nitrogen donor atoms), *cis* and *trans* configurations or different orientations of the imidazole rings from histidine (for example, rings perpendicular or parallel to the square plane of the complex; Dikanov et al., 1994a) might account for two very similar type 2 Cu^{2+} sites.

It is assumed that pMMO is formed from one pmoA (27 kDa), one pmoB (47 kDa), and one pmoC (25 kDa), but further studies are needed to define the active molecule. The active site most likely contains Cu^{1+} in the reduced state. The ratio of EPR-detectable Cu^{2+} to total copper determined by atomic absorption for membrane fractions from *M. album* BG8 is ~1:3, and a rough calculation of the ratio of total copper to the concentration of pMMO is 4:1 (Yuan et al., 1998a,b). The ratio of Cu^{2+}:Cu^{+}, as determined from XAS edge analysis of pMMO membranes for *M. capsulatus* (Bath), can be as much as 1:4 (Nguyen et al., 1996).

Much additional work is needed to resolve these questions, but the current model invoking the . . .HXH. . . sequences appears to be one explanation for the EPR data. Another step is to incorporate Cu^{+} into the model. It should be noted that it is difficult to assign structures that include more than a few copper ions, given the limited number of histidines in the protein. For example, a novel tetranuclear copper cluster in histidine-rich nitrous oxide reductase has seven histidines supporting the tetranuclear copper cluster

(Brown et al., 2000). The 27-kDa subunit, pmoA, which is thought to contain the active site (Shiemke et al., 1995), has only three histidines that are conserved, as discussed earlier for pMMO formed from one 27-kDa, one 47-kDa, and one 25-kDa subunit, so it may be that two or more subunits of pMMO supply histidines to form a cluster, possibly trinuclear, for the active site. It is much less clear how pMMO can support two to four catalytic sites and two to four electron transfer sites involving 15–21 coppers as proposed (Nguyen et al., 1994, 1996, 1998).

We thank Hua Yuan for spectra from *M. album* BG8, which were used for comparison with spectra from *M. capsulatus* (Bath).

This work was supported by grants from CAPES-Brazil to SSL, National Institutes of Health (NIH) grant RR01008 for the multifrequency EPR studies, and NIH grant GM21156 (to GRE and SSE) for the ESEEM studies.

REFERENCES

Alvarez-Cohen, L., P. L. McCarty, E. Boulygina, R. S. Hanson, G. A. Brusseau, and H. C. Tsien. 1992. Characterization of a methane-utilizing bacterium consortium that rapidly degrades trichloroethylene and chloroform. *Appl. Environ. Microbiol.* 58:1886–1893.

Arps, P. J., B. S. Speer, Y. M. Kim, and M. E. Lidstrom. 1995. The *mxa*AKL genes of *Methylobacter albus* BG8. *Microbiology.* 141: 2995–3004.

Berson, O., and M. E. Lidstrom. 1997. Cloning and characterization of *corA*, a gene encoding a copper-repressible polypeptide in the type I methanotroph, *Methylomicrobium albus* BG8. *FEMS Microbiol. Lett.* 148:169–174.

Brantner, C. A., L. A. Buchholz, C. C. Remsen, and M. L. P. Collins. 1997. Intracytoplasmic membrane formation in *Methylomicrobium album* BG8 is stimulated by copper in the growth medium. *Can. J. Microbiol.* 43:672–676.

Brantner, C. A., L. A. Buchholz, C. C. Remsen, and M. L. P. Collins. 2000. Isolation of intracytoplasmic membrane from the methanotropic bacterium *Methylomicrobium album* BG8. *Curr. Microbiol.* 40:132–134.

Brown, K., M. Tegoni, M. Prudencio, A. S. Pereira, S. Besson, J. J. Moura, I. Moura, and C. Cambillau. 2000. A novel type of catalytic copper cluster in nitrous oxide reductase. *Nature Struct. Biol.* 7:191–195.

Chan, S. I., H.-H. T. Nguyen, A. K. Shiemke, and M. E. Lidstrom. 1993. The copper ions in the membrane-associated methane monooxygenase. *In* Bioinorganic Chemistry of Copper. K. Karlin and Z. Tyeklár, editors. Chapman and Hall, New York. 184–195.

Cheng, Y. S., J. L. Halsey, K. A. Fode, C. C. Remsen, and M. L. P. Collins. 1999. Detection of methanotrophs in groundwater by the PCR. *Appl. Environ. Microbiol.* 65:648–651.

Chistoserdova, L., M. Kuhn, and M. E. Lidstrom. 1994. Identification of a promoter region for *mxaF* (*moxF*) from the type I methanotroph, *Methylobacter albus* BG8. *FEMS Microbiol. Lett.* 121:343–348.

Collins, M. L. P., L. A. Buchholz, and C. C. Remsen. 1991. Effect of copper on *Methylomonas albus* BG8. *Appl. Environ. Microbiol.* 57: 1261–1264.

Dikanov, S. A., I. Felli, M.-S. Viezzoli, A. Spoyalov, and J. Huttermann. 1994a. X-band ESEEM spectroscopy of ^{15}N substituted native and inhibitor-bound superoxide dismutase. *FEBS Lett.* 345:55–60.

Dikanov, S. A., A. P. Spoyalov, and J. Huttermann. 1994b. Exploiting the properties of lineshape singularities in orientationally selected electron spin echo envelope modulation spectra of $Cu^{2+}(^{15}N\text{-imidazole})_4$ for the determination of hyperfine coupling with the remote imidazole nitrogen. *J. Chem. Phys.* 100:7973–7983.

Dikanov, S. A., and Y. D. Tsvetkov. 1992. Electron Spin Echo Envelope Modulation (ESEEM) Spectroscopy. CRC Press, Boca Raton, FL.

DiSpirito, A. A., J. Gulledge, A. K. Shiemke, J. C. Murrell, M. E. Lidstrom, and C. L. Krema. 1992. Trichloroethylene oxidation by the membrane-associated methane monooxygenase in type I, type II, and type X methanotrophs. *Biodegradation.* 2:151–164.

Drought, J. F., E. A. Buc, T. J. Grundl, K. A. Fode, and M. L. P. Collins. 1999. Fate of tetrachloroethene and benzene at a dry cleaning facility. *In* Proceedings of the 5th in Situ and On-Site Bioremediation Symposium. Batelle Press. Columbus, OH. 253–258.

Elliott, S. J., D. W. Randall, R. D. Britt, and S. I. Chan. 1998. Pulsed EPR studies of particulate methane monooxygenase from *Methylococcus capsulatus* (Bath): evidence for histidine ligation. *J. Am. Chem. Soc.* 120:3247–3248.

Elliott, S. J., M. Zhu, L. Tso, H.-H. T. Nguyen, J. H.-K. Yip, and S. I. Chan. 1997. Regio- and stereoselectivity of particulate methane monooxygenase from *Methylococcus capsulatus* (Bath). *J. Am. Chem. Soc.* 119: 9949–9955.

Fee, J. A., J. Peisach, and W. B. Mims. 1981. Superoxide dismutase: examination of the metal binding sites by electron spin echo spectroscopy. *J. Biol. Chem.* 256:1910–1914.

Fode, K. A., C. Wimpee, C. C. Remsen, and M. L. P. Collins. 1999. Direct application of PCR to environmental samples. *In* Abstracts of the General Meeting of the American Society for Microbiology. 572.

Hanson, R. S., and T. E. Hanson. 1996. Methanotrophic bacteria. *Microbiol. Rev.* 60:439–471.

Holm, R. H., P. Kennepohl, and E. I. Solomon. 1996. Structural and functional aspects of metal sites in biology. *Chem. Rev.* 96:2239–2314.

Holmes, A. J., A. Costello, M. E. Lidstrom, and J. C. Murrell. 1995. Evidence that particulate methane monooxygenase and ammonia monooxygenase may be evolutionarily related. *FEMS Microbiol. Lett.* 132: 203–208.

Iwata, S., C. Ostermeier, B. Ludwig, and H. Michel. 1995. Structure at 2.8 Å resolution of cytochrome *c* oxidase from *Paracoccus denitrificans. Nature.* 376:660–669.

Lipscomb, J. D. 1994. Biochemistry of the soluble methane monooxygenase. *Annu. Rev. Microbiol.* 48:371–399.

Little, C. D., A. V. Palumbo, S. E. Herbes, M. E. Lidstrom, R. L. Tyndall, and P. J. Gilmer. 1988. Trichloroethylene biodegradation by a methane-oxidizing bacterium. *Appl. Environ. Microbiol.* 54:951–956.

Lontoh, S., and J. D. Semrau. 1998. Methane and trichloroethylene degradation by *Methylosinus trichosporium* OB3b expressing particulate methane monooxygenase. *Appl. Environ. Microbiol.* 64:1106–1114.

Lu, J., C. J. Bender, J. McCracken, J. Peisach, J. C. Severns, and D. R. McMillin. 1992. Pulsed EPR studies of the type 2 copper binding site in the mercury derivative of laccase. *Biochemistry.* 31:6265–6272.

McPheat, W. L., N. H. Mann, and H. Dalton. 1987. Isolation of mutants of the obligate methanotroph *Methylomonas albus* defective in growth on methane. *Arch. Microbiol.* 148:40–43.

Messerschmidt, A. 1993. Ascorbate oxidase structure and chemistry. *In* Bioinorganic Chemistry of Copper. K. D. Karlin and Z. Tyeklár, editors. Chapman and Hall, New York. 459–470.

Mims, W. B. 1984. Elimination of the dead-time artifact in electron spin-echo envelope spectra. *J. Magn. Reson.* 59:291–306.

Mims, W. B., and J. Peisach. 1978. The nuclear modulation effect in electron spin echoes for complexes of Cu^{2+} ion and imidazole with nitrogen-14 and nitrogen-15. *J. Chem. Phys.* 69:4921–4930.

Nguyen, H.-H. T., S. J. Elliott, J. H.-K. Yip, and S. I. Chan. 1998. The particulate methane monooxygenase from *Methylococcus capsulatus* (Bath) is a novel copper-containing three-subunit enzyme. *J. Biol. Chem.* 273:7957–7966.

Nguyen, H.-H. T., K. H. Nakagawa, B. Hedman, S. J. Elliott, M. E. Lidstrom, K. D. Hodgson, and S. I. Chan. 1996. X-ray absorption and EPR studies on the copper ions associated with particulate methane monooxygenase from *Methylococcus capsulatus* (Bath). Cu(I) ions and their implications. *J. Am. Chem. Soc.* 118:12766–12776.

Nguyen, H.-H. T., A. K. Shiemke, L. J. Jacobs, B. J. Hales, M. E. Lidstrom, and S. I. Chan. 1994. The nature of the copper ions in the membranes

containing the particulate methane monooxygenase from *Methylococcus capsulatus* (Bath). *J. Biol. Chem.* 269:14995–15005.

Oldenhuis, R., J. Y. Oedzes, J. J. van der Waarde, and D. B. Janssen. 1991. Kinetics of chlorinated hydrocarbon degradation by *Methylosinus trichosporium* OB3b and toxicity of trichloroethylene. *Appl. Environ. Microbiol.* 57:7–14.

Rakhit, G., W. E. Antholine, W. Froncisz, J. S. Hyde, J. R. Pilbrow, and G. R. Sinclair. 1985. Direct evidence of nitrogen coupling in copper(II) complex of bovine serum albumin by S-band electron spin resonance technique. *J. Inorg. Biochem.* 25:217–224.

Rosenzweig, A. C., C. A. Frederick, S. J. Lippard, and P. Nordlund. 1993. Crystal structure of a bacterial non-human iron hydroxylase that catalyses the biological oxidation of methane. *Nature.* 366:537–543.

Semrau, J. D., A. Chistoserdov, J. Lebron, A. Costello, J. Davagnino, E. Kenna, A. J. Holmes, R. Finch, J. C. Murrell, and M. E. Lidstrom. 1995a. Particulate methane monooxygenase genes in methanotrophs. *J. Bacteriol.* 177:3071–3079.

Semrau, J. D., D. Zolandz, M. E. Lidstrom, and S. I. Chan. 1995b. The role of copper in the pMMO of *Methylococcus capsulatus* (Bath) a structural vs. catalytic function. *J. Inorg. Biochem.* 58:235–244.

Shiemke, A. K., S. A. Cook, T. Miley, and P. Singleton. 1995. Detergent solubilization of membrane-bound methane monooxygenase requires plastoquinol analogs as electron donors. *Arch. Biochem. Biophys.* 321: 421–428.

Takeguchi, M., K. Fukui, H. Ohya, and I. Okura. 1999. Electron spin-echo envelope modulation studies on copper site of particulate methane monooxygenase from *Methylosinus trichosporium* OB3b. *Chem. Lett.* No. 7, July:617–618.

Takeguchi, M., K. Miyakawa, and I. Okura. 1998a. Properties of the membranes containing the particulate methane monooxygenase from *Methylosinus trichosporium* OB3b. *Biometals.* 11:229–234.

Takeguchi, M., K. Miyakawa, and I. Okura. 1998b. Purification and properties of particulate methane monooxygenase from *Methylosinus trichosporium* OB3b. *J. Mol. Catalysis A Chem.* 132:145–153.

Vänngård, T. 1972. Copper proteins. *In* Biological Applications of Electron Spin Resonance. H. M. Swartz, J. R. Bolton, and D. C. Borg, editors. Wiley-Interscience, New York. 425–432.

Whittenbury, R., K. C. Phillips, and J. F. Wilkinson. 1970. Enrichment, isolation, and some properties of methane-utilizing bacteria. *J. Gen. Microbiol.* 61:205–218.

Wilce, M. C. J., D. M. Dooley, H. C. Freeman, J. M. Guss, H. Matsunami, W. S. McIntire, C. E. Ruggiero, K. Tanizawa, and H. Yamaguchi. 1997. Crystal structures of the copper-containing amine oxidase from *Arthrobacter globiformis* in the holo and apo forms: implications for the biogensis of topaquine. *Biochemistry.* 36:16116–16133.

Yuan, H., M. L. P. Collins, and W. E. Antholine. 1997. Low frequency EPR of the copper in particulate methane monooxygenase from *Methylomicrobium albus* BG8. *J. Am. Chem. Soc.* 119:5073–5074.

Yuan, H., M. L. P. Collins, and W. E. Antholine. 1998a. Concentration of Cu, EPR-detectable Cu, and formation of cupric-ferrocyanide in membranes with pMMO. *J. Inorg. Biochem.* 72:179–185.

Yuan, H., M. L. P. Collins, and W. E. Antholine. 1998b. Analysis of type 2 Cu(2+) in pMMO from *M. album* BG8. *Biophys. J.* 74:A300.

Yuan, H., M. L. P. Collins, and W. E. Antholine. 1999. Type 2 Cu(2+) in pMMO from *Methylomicrobium album* BG8. *Biophys. J.* 76:2223–2229.

Zahn, J. A., and A. A. DiSpirito. 1996. Membrane-associated methane monooxygenase from *Methylococcus capsulatus* (Bath). *J. Bacteriol.* 178:1018–1029.

Zhou, Y., B. E. Bowler, G. R. Eaton, and S. S. Eaton. 1999. Electron spin lattice relaxation rates for $S = 1/2$ molecular species in glassy matrices or magnetically dilute solids at temperatures between 10 and 300 K. *J. Magn. Reson.* 139:165–174.